Thermophoresis of a colloidal rod: contributions of charge and grafted polymers

Zilin Wang,[†] Doreen Niether,[†] Johan Buitenhuis,[†] Yi Liu,[†] Peter R. Lang,[†] Jan K.G. Dhont,[†,‡] and Simone Wiegand[*,†,¶]

[†]*ICS-3 Soft Condensed Matter, Forschungszentrum Jülich GmbH, D-52428 Jülich, Germany*

[‡]*Department of Physics, Heinrich-Heine-Universität Düsseldorf, D-40225 Düsseldorf, Germany*

[¶]*Department für Chemie - Physikalische Chemie, Universität zu Köln, 50939 Cologne, Germany*

E-mail: s.wiegand@fz-juelich.de

Abstract

In this study we investigated the thermodiffusion behavior of a colloidal model system as function of Debye length, λ_{DH}, which is controlled by the ionic strength. Our system consists of an *fd*-virus grafted with polyethylene glycol (PEG) with a molecular mass of 5000 g/mol. The results are compared with recent measurements on bare *fd*-virus and results of PEG. The diffusion coefficients of both viruses are comparable and increase with increasing Debye length. The thermal diffusion coefficient, D_{T}, of the bare virus increases strongly with the Debye length, while D_{T} of the grafted *fd*-virus shows only a very weak increase. The Debye length dependence of both systems can be described with an expression derived for charged rods using the surface charge density and an offset of D_{T} as adjustable parameters. It turns out that the ratio of the

determined surface charges is inverse to the ratio of the surfaces of the two systems, which means that the total charge remains almost constant. The determined offset of the grafted *fd*-virus describing the chemical contributions is the sum of D_{T} of PEG and the offset of the bare *fd*-virus. At high $\lambda_{\mathrm{D}H}$, corresponding to low ionic strength, the S_{T}-values of both colloidal model systems approach each other. This implies a contribution from the polymer layer, which is strong at short $\lambda_{\mathrm{D}H}$ and fades out for the longer Debye lengths, when the electric double layer reaches further than the polymer chains and therefore dominates interactions with the surrounding water.

Keywords

Thermodiffusion, Soret-effect, polyethlene glycol, Debye length, diffusion, hydration, fd-virus

February 4, 2019

Introduction

In the last five years, thermodiffusion has gained a lot of interest due to applications in biotechnology[1] and as one key parameter in the origin of life puzzle.[2,3] Thermophoresis describes a mass separation induced by a temperature gradient in a multi-component system. The achieved separation of the mixture under a temperature gradient is quantified by the Soret coefficient $S_{\mathrm{T}} = D_{\mathrm{T}}/D$, where D_{T} is the thermal diffusion coefficient and D is the mass diffusion coefficient.

Thermodiffusion and thermophoresis has been studied experimentally,[4–9] theoretically[10–13] and by computer simulations.[14–19] The studies cover many different systems such as low molar mass mixtures, polymer solutions, microemulsions and colloidal dispersions. Recent simulations by Tan and Ripoll elucidate especially the changes of the thermophoretic motion of rod-like particles.[19] Even in simple non-polar liquid mixtures there is still a lack of deep microscopic understanding of thermodiffusion although for those systems the thermophoretic

behavior can be predicted to some extent by using thermodynamic concepts such as heats of transfer or empirical equations.[20–22] Due to the complexity of interactions introduced by hydrogen bonds and long range charge effects, the behavior of aqueous systems is often even less predictable. The direction and amplitude of the thermophoretic motion depends on a number of properties such as size, charge, hydration shell and conformation, which are influenced by temperature and composition changes.

Important contributions to the thermophoretic behavior of aqueous systems are changes in the hydration layer and charge effects. Changes due to differences in the hydration of the solute molecules are mainly reflected in the temperature sensitivity of the Soret coefficient.[6,23–25] Recent systematic studies of sugar and amide systems[26,27] showed that the hydrophilicity of the solute compound plays an important role. For many uncharged systems it was found that the temperature sensitivity of the Soret coefficient is related to the so called partition coefficient $\log P$,[28] which is a qualitative measure for the hydrophilicity. The general trend is that in the dilute regime more hydrophilic compounds show a stronger increase of S_T with temperature. For solutes with stronger hydrophobic contribution, such as ethanol,[29] DMSO[30] and crown ether,[31] a decrease of S_T with increasing temperature has been observed. An increase of the solute concentration above a certain threshold has also been shown to lead to a decay of S_T with increasing T. Molecular dynamic simulations of urea in water show that an artificial increase of the hydrophilicity can reverse the temperature dependence at high solute concentrations.[25] At the present state of knowledge, we can state that the typical increase of S_T with temperature is only observed, if the solute molecules form strong hydrogen bonds with water.

Beside the hydration effects, charge contributions to the thermophoresis of salts and colloids have been studied extensively by experiment,[7,9,32–34] theory[10,13,35–40] and simulations.[16–18,41] Some of the theoretical approaches consider thermoelectric effects generated by the cloud of counter-ions,[37,38] while others consider the thermophoretic force on the charged colloidal particle due to the presence of its double layer.[36,36,40] Sehnem *et al.* could describe

the temperature dependence of the experimental Soret coefficient of a ferrofluid by using a combination of both approaches.[34] For charged rods we have only the theoretical model by Dhont. To describe charged rods he extended his theory for charged spheres[35,36] by constructing a rod as "shish-kebab" model built by connected beads in a linear disposition. In this approach we have two adjustable parameters: the surface charge density and an offset describing the chemical contribution. It was possible to describe experimental thermophoresis data of a bare *fd*-virus with this model[33] and the calculated surface charge density was in agreement with electrophoretic measurements. In conclusion we can state that a convincing theoretical concept exists, if the electric double layer contributions to the thermophoretic behavior dominate those of other, more short range, interactions.

The main advantage of the colloidal systems compared to other soft materials is that the number of degrees of freedom are reduced, which simplifies the theoretical modeling.[42,43] In the past years, colloidal particles and soft colloids such as microemulsions have also been used as model systems to develop and to validate theoretical predictions of thermophoresis as function of size, charge, interfacial tension and temperature.[7,8,32,33,44–49]

In this study we investigate how the thermophoretic behavior changes when we graft electrostatically neutral polyethylene glycol (PEG) chains on the bare *fd*-virus. Note that in the literature often the synonymous name polyethylene oxide (PEO) has been used.[50,51] Grafting or adsorption of polymers is of general interest and typically influences the phase behavior, the stability of suspensions, the diffusion and also the interaction potential. In the past, the majority of studies dealt with spherical colloids,[52–55] but also the rod-like *fd*-virus has been studied extensively.[56–58] The wild type *fd*-virus has a molar mass of 1.64×10^7 g/mol, a contour length L of 880 nm, a radius a of 3.4 nm, and a persistence length L_P of 2.2 μm. The *fd*-virus consist of a single-strand DNA, coated with amino groups and acidic residues, which determine the surface properties of the *fd*-virus. Above pH 4 the virus is negatively charged and interacts via a combination of electrostatic repulsion and hard-core interactions. The net surface charge can be increased or decreased by increasing or decreasing the solution

pH, respectively.[59] Therefore, the *fd*-virus can be electrostatically stabilized by adjusting the pH value or the ionic strength of the solution. However, the change of ionic strength will always modify the effective thickness of the electric double layer, which has an influence on the effective volume of the *fd*-virus.

The thermophoretic behavior of bare *fd*-virus was measured as function of the rod-concentration and Debye screening length by tuning the buffer concentration.[32,33] The Soret coefficient of the rods increased with increasing Debye length, with either fixed and varied rod-concentration.[33] Meanwhile, it shows almost no dependence on the rod-concentration when the ionic strength is kept constant. When the effective volume fraction of the rods is fixed by varying simultaneously the ionic strength and rod-concentration, the Soret coefficient still shows an increasing dependence on Debye length (cf. fig. 5 in Ref.[33]). In conclusion, the thermophoretic motion of the bare *fd*-virus is predominantly determined by the contribution of the electric double layer.

The thermodiffusion behavior of PEG has been investigated independently by different experimental techniques.[50,51,60–62] Among the water soluble polymers PEG is of special interest due to its complex phase behavior in water, which is caused by a delicate balance of opposing effects,[63,64] leading to mixing at low temperatures and demixing at high temperatures.

For this work surface modification of the *fd*-virus was achieved by using PEG with an active *N*-hydroxysuccinimide (NHS) end. The grafting of PEG to the surface of the virus results primarily in steric changes (an increase of the virus surface), but can also change chemical interactions between surface and solvent. We expect that these modifications affect colloid-solvent interactions at high ionic strengths, because the electric double layer is then relatively short-ranged and therefore deeply confined within the grafted polymers. At low ionic strength the interaction is expected to be determined by the electric double layer, as intuitively illustrated by Figure 1. To support our hypothesis we perform systematic thermophoretic measurements as function of the ionic strength in order to tune the interactions

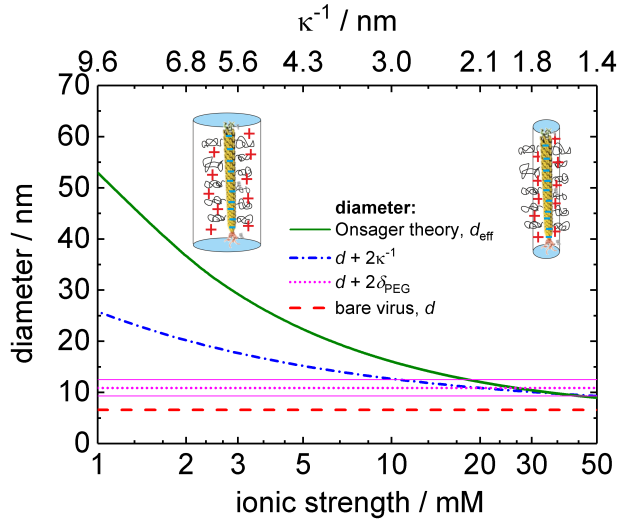

Figure 1: (Color online) The cartoons illustrate our assumption that at low ionic strength the system is dominated by charge effects, while at high ionic strength the steric repulsion should rule the system. To support this hypothesis various diameters are plotted as function of the ionic strength: d is the bare diameter of the *fd*-virus (dashed red line), $d + 2\delta_{\mathrm{PEG}}$ is the bare diameter plus the thickness of the grafted PEG layer (dotted magenta line with thin magenta lines marking uncertainty), $d + 2\kappa^{-1}$ is the bare diameter plus two times the Debye length (dash-dotted blue line), and d_{eff} is the effective diameter of the charged rod according to the Onsager theory[65] (solid green line).

from steric to charge dominated.

Zhang *et al.*, who investigated the liquid-crystalline phase behavior of *fd*-virus with PEG chains of a molar mass of 5000 g/mol, found that the phase behavior of PEG-*fd*-virus starts to become ionic strength independent above 20 mM, corresponding to a Debye length of 2.15 nm, because under this high ionic strength the electric double layer is confined within the PEG layer. Below the ionic strength of 20 mM the dominant interaction should be electrostatic.[66] The thickness of the grafted PEG layer is estimated as $\delta_g^{\mathrm{PEG}} = 4.3 \pm 1.6$ nm based on several experiments (details are explained in SI (Section S1)). Calculation of the effective diameter of the rod d_{eff} according to the Onsager theory also indicates a dominance of the charge contribution below an ionic strength of 20mM (cf. fig. 1; details are explained in SI (Section S2)), which is in agreement with the observed phase behavior.

This paper is organized as follows. First, we discuss an heuristic approach to describe

the thermophoresis of charged rods with steric stabilization layer. Then we describe the preparation and characterization of PEG grafted *fd*-virus. In the results and discussion section we present experimental measurements of the thermodiffusion of PEG grafted *fd*-virus in comparison with the bare *fd*-virus. The main conclusions and final remarks close the paper.

Heuristic approach for charged colloidal rods with steric stabilization

In the following we will elucidate the physical forces acting on a charged colloidal rod with a steric stabilization layer as sketched in figure 2. For simplicity we aligned the rod in the direction of the temperature gradient, but depending on its relative orientation the forces acting on the rod will vary.[19] First, there is a pressure difference between the warm and the cold side, which is also influenced by the collective interactions between colloidal particles and hydrodynamic forces on the colloids.[11,67] Secondly, there are charge effects leading to a force acting on the colloidal particles,[35–37] which can be outweighed by steric interactions in the case of thin Debye layers.

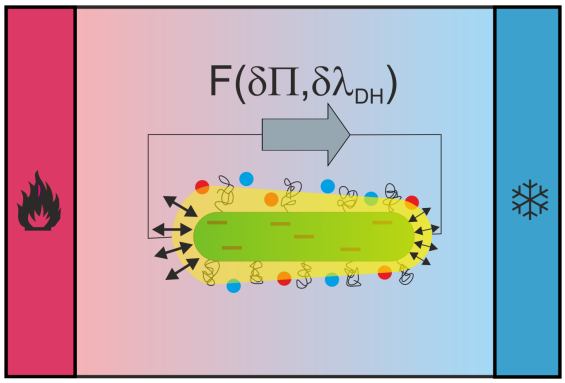

Figure 2: (Color online) Illustration of a charged rod in a temperature gradient and the forces acting on it. Drawing not to scale.

In the case of spheres the concentration dependence of the collective diffusion D and the

thermal diffusion coefficient D_{T} neglecting hydrodynamic interactions are given by,

$$\begin{aligned} D &= D_0 \beta \frac{\partial \Pi\left(\rho, T, \mu_s\right)}{\partial \rho} \\ D_{\mathrm{T}} &= \frac{V_c^0 D_0 \beta}{\phi\left(1-\phi\right)} \frac{\partial \Pi\left(\rho, T, \mu_s\left(T, s\right)\right)}{\partial T}, \end{aligned} \tag{1}$$

where $D_0 = k_B T/\gamma$ is Einstein's translational diffusion coefficient for non-interacting spheres, T the temperature, μ_s the chemical potential of the solvent, ρ the number density, Π the osmotic pressure, k_B Boltzmann's constant, ϕ the volume fraction, V_c^0 the geometric volume of a single colloidal particle and $\beta = 1/k_B T$.[11,68] In the case of interacting spheres in small temperature gradients analytical expressions can be derived.[11,67] Unfortunately the calculation of the concentration dependence of the diffusion of rods is an unsolved analytical problem,[69] so that we suggest a virial expansion like expression to describe the collective contribution of the thermal diffusion coefficient.

$$D_{\mathrm{T}}^{\phi} \approx \frac{D_0}{T}\left[1 + B_x \phi\right]. \tag{2}$$

The first term within the square brackets for D_{T}^{ϕ} is the "ideal gas" and B_x is an adjustable parameters describing the concentration dependence. Note that in the case of colloidal spheres B_x equals B_2, the second virial coefficient. As we will see later the "ideal gas"-term D_0/T is two orders of magnitude smaller than the measured thermal diffusion coefficients and can be neglected.

Beside the concentration dependence, we have an ionic contribution, which has been calculated for highly dilute solutions of charged colloids.[36] Ignoring the contribution due to the non-spherical symmetry of the double layer structure and the resulting solvent flow, which is only important in the case of solvents with low dielectric constants, we find for a

charged rod with length L and radius a

$$D_{\mathrm{T}}^{\mathrm{charge}} = \frac{D_0}{T}\left\{\frac{1}{4}\left(\frac{L}{2a}\right)\left(\frac{4\pi\lambda_{Bj}^2\sigma}{e}\right)^2\left(\frac{a}{\lambda_{Bj}}\right)^3\frac{\kappa a}{(1+\kappa a)^2}\right. \\ \left.\times\quad\left[1-\frac{d\ln\varepsilon}{d\ln T}\left(1+\frac{2}{\kappa a}\right)\right]\right\}+A(T) \tag{3}$$

where σ is the surface charge density, κ^{-1} the Debye length, $\lambda_{Bj} = \beta e^2/4\pi\epsilon$ is the Bjerrum length (0.71 nm for water at room temperature), ε is the permittivity of water at ambient temperature, and $A(T)$ is the additive contribution from the solvation layer and the core material of the colloid, which is treated as an adjustable parameter. The Stokes-Einstein translational diffusion coefficients for the bare *fd*-virus[70] and PEG-*fd*-virus are equal to $D_0 = 2.25\times10^{-8}$ cm^{2}s^{-1} and $D_0 = 2.1\times10^{-8}$ cm^{2}s^{-1}, respectively (for details see SI). In order to describe the total thermal diffusion coefficient $D_{\mathrm{T}}^{\mathrm{total}}$ we use the sum of Eqs. 2 and 3.

$$D_{\mathrm{T}}^{\mathrm{total}} = D_{\mathrm{T}}^{\phi} + D_{\mathrm{T}}^{\mathrm{charge}} \tag{4}$$

Note that at a Debye length of $\kappa^{-1} = 0$ at high salt content the term in the curly bracket in eq.3 equals zero, so that in the low concentration limit with $B_x\phi \approx 0$ the thermal diffusion coefficient is given by

$$D_{\mathrm{T}}^{\mathrm{total}} = \frac{D_0}{T} + A(T). \tag{5}$$

As mentioned before for our system D_0/T can be neglected, so that at $\kappa^{-1} = 0$ the thermal diffusion coefficient is dominated by the offset $A(T)$.

Experimental Details

Sample Preparation and Characterization

The *fd*-virus was prepared following a standard biological protocol using XL1-Blue strain of *E. coli* as the host bacteria.[71] The obtained virus was purified by repetitive centrifugation

(108000 g) and then re-dispersed in 2 mM Tris(hydroxymethyl)aminomethane (Tris) buffer solution.

PEG grafted *fd*-viruses (PEG-*fd*) were prepared using PEG with an activated succinimidyl end-group (Methoxypolyethylene glycol 5000 propionic acid N-succinimidyl ester (mPEG-SPA) obtained from Fluka) which reacts with the amino groups on the surface of the virus following Dogic *et al.*[72] with some minor modifications. As the succinimidyl-groups would also react with the amine group of the Tris buffer, the virus described above was transferred to a 20 mM phosphate buffer at pH 8.5 with 15% ethanol to prevent the growth of micro-organisms. The virus solution was diluted with buffer to obtain about 215 mL *fd* solution of 4 mg/mL. Then 4.1 g of solid mPEG-SPA polymer was added to the stirring solution of the virus and the reaction was allowed to proceed for a few hours. After that the virus was purified from the excess unreacted PEG by three centrifugation/redispersion cycles at 30000 rpm (about 108000 g at the bottom of the tubes) to obtain a stock solution of PEG-*fd* in a 2 mM Tris/1 mM HCl buffer (pH 8.1).

The successful PEG grafting on the *fd*-virus was demonstrated by the difference of the concentration at which the isotropic nematic (IN) phase transition takes place for PEG-*fd* as compared to bare *fd* at an ionic strength of 100 mM.[72] For this a small amount of bare *fd* and PEG-*fd* were redispersed in a 200 mM Tris/100 mM HCl buffer (pH 8.3, ionic strength 100 mM) by repeated centrifugation/redispersion cycles as described above. The concentrated virus dispersions were diluted with buffer drop by drop until the permanent birefringence was just lost. From these solutions the concentration was determined by the UV absorption at 269 nm, using an absorption coefficient of 3.84 $\mathrm{cm^2 mg^{-1}}$. The PEG itself was found not to contribute significantly to the absorption at 269 nm, so that for PEG-*fd* the concentration of the *fd* core is obtained. In this way an IN phase transition concentration of 9 mg/mL was obtained for the PEG-*fd*, whereas for bare *fd* the corresponding concentration was found to be 19 mg/mL. This large difference in concentration indicates a higher grafting density as compared to the original results from Dogic.[72]

To characterize the grafting density more quantitatively, the concentration obtained from the solid content was compared to the concentration from the UV absorption. Because the solid content includes the weight of the PEG whereas the UV absorption only measures the corresponding concentration of the *fd* cores (PEG does not absorb significantly) the amount of PEG grafted to the virus can be determined from the difference of solid content to the 'UV-concentration'. Because PEG continuous to lose mass if dried at higher temperatures, the solid content was determined at a moderate temperature of 35°C under vacuum. All masses were obtained by drying to constant weight, drying bottles were pre-dried to obtain their empty weight and the small contribution of TRIS was determined and subtracted. In this way the solid content was determined twice using about 13 mg dry PEG-*fd* per determination. Doing so resulted in an approximate value of 22 wt% PEG relative to the *fd* part of PEG-*fd*, or 18 wt% PEG relative to the weight of PEG-*fd*. Using a molar mass of 16.4×10^6 g/mol for the *fd*-virus, 5000 g/mol for the PEG and 2700 major coat proteins per virus, this corresponds to about 27% of coat proteins being grafted with a PEG molecule.

Tris with concentrations of 82.15, 29.57, 15.09, 6.11, 3.29, and 2.05 mM were used as buffer solutions. The pH of all buffer solutions was adjusted to 8.2 by adding concentrated hydrochloric acid (HCl) solution. The stock solution of PEG-*fd*-virus was dialyzed in each chosen buffer and then the concentration was adjusted to 1 mg/ml. As previous measurements showed no concentration dependence of the thermal diffusion coefficient between 1-3 mg/mL,[32] we studied only the lowest concentration, well below the semi-dilute regime starting at 8 mg/mL. Concentrations were determined by UV absorption (NanoDrop ND-1000, Peqlab). All measurements have been performed at 20°C.

The Einstein diffusion coefficient D_0 was measured in the dilute limit by dynamic light scattering (see SI section S4 for details).

Electrophoresis experiments

In order to compare the total charge of the bare virus and the PEG-*fd*-virus we measured the electrophoretic mobility on a Malvern Zetasizer 2000 in a M3 capillary cell. For all measurements the applied electrical field strength was about 30 V/cm, which is well below the field strengths necessary for a significant field-induced orientation of the viruses at the 0.1 mg mL^{-1} concentration.[73] Before the measurements, all samples were filtered through a 5 μm nylon filter. The cell was rinsed with filtered solution and carefully checked for air bubbles before measurements. Each measurement had been repeated at least 3-times. The measurements were checked for reproducibility, due to their sensitivity to bubbles or dust. Care was taken to allow for enough waiting time between the runs. All measurements were performed at 25°C.

Solutions of the bare *fd*-virus and PEG-*fd*-virus with the same ionic strength were used to measure electrophoresis. Both viruses have been measured at two concentrations (0.1 and 1 mg/mL) at the same ionic strength of 4 mM TrisHCl buffer at a pH of 8.2. At the low concentration of 0.1 mg/mL we measured an electrophoretic mobility of -3.22 ± 0.16 $\mu mVs^{-1}cm^{-1}$ for the bare and -1.42 ± 0.08 $\mu mVs^{-1}cm^{-1}$ for the PEG-*fd* virus. For the higher concentration of 1 mg/mL we obtained -3.98 ± 0.02 $\mu mVs^{-1}cm^{-1}$ and -2.10$\pm$0.03 $\mu mVs^{-1}cm^{-1}$. For both concentrations the absolute values of electric mobility are smaller for PEG-*fd* than for the bare *fd*-virus. To exclude the interactions between rods, the electric mobility is divided by diffusion coefficient D, but the normalized mobility of the bare *fd*-virus remains roughly 50% larger compared to PEG-*fd*-virus.

Solely on the basis of the higher mobility measured for the bare *fd*-virus we can not conclude that the charge is higher compared to that of the PEG-*fd*-virus, because the electrophoretic mobility is also influenced by the movement of counter ions in opposite direction. In the case of PEG-*fd*-virus the movement of counter ions might be hindered by the polymer chains, which would lead to lower mobility even with the same surface charge. There are two mechanism which can change the charge due to the presence of PEG chains. *First*,

the dissociation of the amino groups, which increases the number of positive charges at the surface and leads to a reduction of the net (total) negative charge. As the PEG chains are grafted to the amino groups, less amino groups can dissociate, which reduces the amount of positive charges and leads to an increase of the net negative charge. Note that the pH value decreases from bulk to the surface of the rods according to the Boltzmann equation[74,75]

$$[\mathrm{H}^+]_{\mathrm{surface}} = \left[\mathrm{H}^+\right]_{\mathrm{bulk}} \cdot \exp\left(-e\psi_0/k_BT\right), \tag{6}$$

with e being the elementary charge, k_B the Boltzmann constant and ψ_0 the electrostatic surface potential. For bare fd at a bulk pH of 8.2 and an ionic strength of 1mM the surface pH is calculated as 5.25, corresponding to 100% ionization of the -NH_2 groups, whereas the carboxyl groups are ionized to about 85%. Since 27% of the coat proteins are grafted with PEG, the number of amino groups per coat protein changes from 2 to 1.73, and the net negative charge increases at most by about 10%.[75] The *second* mechanism leading to a change of the surface charge is a reduction of the dielectric constant ϵ of the water layer surrounding the virus due to the presence of PEG chains. This will lead to an increase of the Bjerrum length and the same relative reduction of the line charge density. Consequently, taking into account the relative volume occupied by the PEG chains, we expect a reduction of the total negative charge in the order of 5-10%. In conclusion, the smaller number of dissociating surface groups and the reduction of the dielectric constant due to the grafting of the polymer leads to a similar increase and decrease of the absolute surface charge by approximately 5-10%, respectively. So that, we assume for further considerations that the total charge of PEG grafted *fd*-virus is the same as that of bare *fd*-virus.

Infrared Thermal Diffusion Forced Rayleigh Scattering (IR-TDFRS)

All thermodiffusion measurements were performed with Infrared Thermal Diffusion Forced Rayleigh Scattering (IR-TDFRS). A detailed description of the IR-TDFRS can be found

Table 1: Adjusted parameters (surface charge σ and offset $A(T)$) according to Eq.3 displayed in figure 3.

system	σ/e nm^{-2}	$A(T)$ / 10^{-8}cm^{2}s^{-1}
bare *fd*-virus	0.051 ± 0.002	-2.4 ± 0.4
PEG-*fd*-virus	0.020 ± 0.004	3.2 ± 0.4

in the literature.[32,33] Measurement of the refractive index contrast factors with respect to mass concentration at constant pressure and temperature $(\partial n/\partial c)_{p,T}$, and with respect to temperature at constant pressure and mass concentration $(\partial n/\partial T)_{p,c}$ has also been described in earlier works.[33]

Results and Discussion

We investigated the thermophoretic behavior of PEG grafted *fd*-virus as a function of ionic strength in the range between 1 mM and 41 mM. According to Zhang *et al.*[66] we expect the behavior of PEG-*fd* to be similar to that of bare *fd*-virus at low ionic strength. As sketched in cartoon (fig. 1) the physical picture is that the electrostatic double layer reaches further than the PEG-chains, thus dominating interactions.

In Figure 3 the obtained D and D_{T}-values of PEG-*fd* and bare *fd*-virus are shown as function of the Debye length. The corresponding Stokes-Einstein translational diffusion coefficient D_0 in the dilute limit at $\kappa^{-1} \approx 0$ are $D_0 = (2.1 \pm 0.4) \times 10^{-8}\mathrm{cm}^2\mathrm{s}^{-1}$ and $D_0 = (2.25 \pm 0.05) \times 10^{-8}\mathrm{cm}^2/\mathrm{s}$ for PEG-*fd* and *fd*, respectively. They agree within their error bars (further details are given in the SI section S4). For both systems D increases with increasing Debye length, corresponding to lower salt content. The observation that the collective diffusion slows down with decreasing Debye length is in agreement with observations made for spheres.[76,77]

The lower graph of figure 3 shows that the thermal diffusion coefficient D_{T} of PEG-*fd*

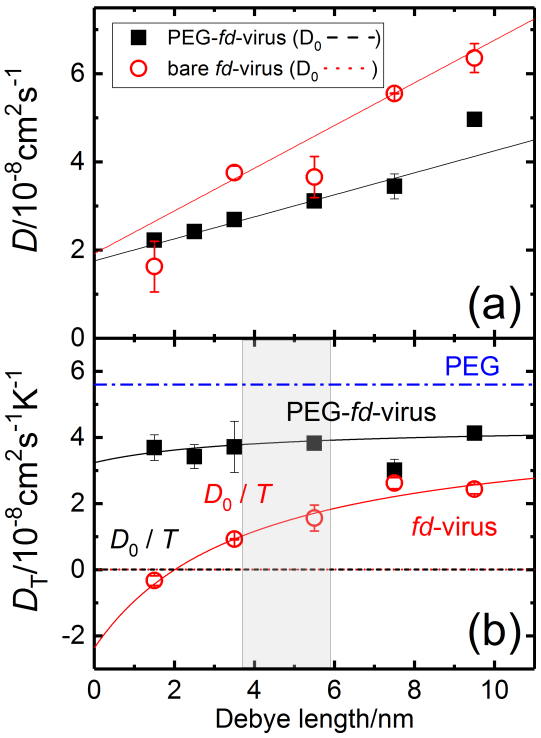

Figure 3: Diffusion coefficient D (a) and thermal diffusion coefficient D_{T} (b) as function of the Debye length. Shown are the PEG-*fd*-virus (black squares) and bare *fd*-virus (red circles) at a concentration of 1 mg/mL. The solid lines are linear fits (a) and fits according to the sum of Eqs. 2 and 3 with $B_x = 0$ (b). The "ideal gas"-terms D_0/T are shown as dashed black and dotted red line. Note that they are both very close to zero and seem to lie on top of each other in the scale of the graph. The shaded area marks where the Debye length equals the thickness of the grafting layer. The blue dashed-dotted line corresponds to the thermal diffusion coefficient of 2 wt% PEG in water at 25°C.[62]

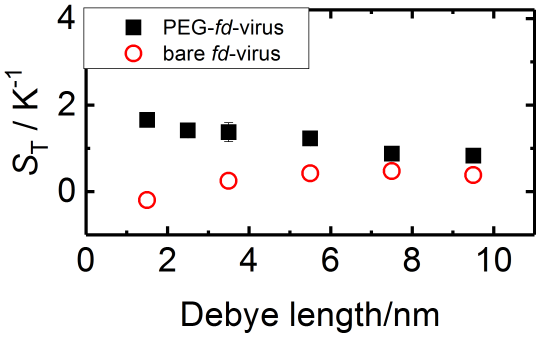

Figure 4: S_{T} of the PEG-*fd*-virus (black squares) and bare *fd*-virus (red circles) at a concentration of 1 mg/mL as function of the Debye length. The errors are indicated by symbol size.

depends only weakly on the Debye length, λ_{DH}, while D_{T} of the bare *fd*-virus increases with increasing Debye length. The Debye length dependence of the thermal diffusion coefficient can be fully described by the sum of Eqs. 2 and 3 with $B_x = 0$, so that we have only two adjustable parameters, the surface charge σ and the offset $A(T)$, which are listed in table 1. As discussed before D_{T} can be approximated by the offset $A(T)$ at $\lambda_{\mathrm{DH}} = 0$, because the "ideal gas"-term D_0/T contributes less than 0.5% to D_{T} (c.f. fig.3(b)). It turns out that the offset $A(T)$ of the PEG-*fd* is roughly equal to the sum of the D_{T}-values of PEG and of the bare *fd*-virus.[33] For this systems we can conclude that the polymeric chains at the surface and the core material of the colloidal rod are in contact with the solvent and contribute to the thermophoretic motion of the hairy colloid. The effective surface charge σ of the bare *fd*-virus is roughly a factor 2.5 larger than that of the PEG-*fd*, which corresponds to the inverse surface ratio $a/(a + \delta_{\mathrm{PEG}}) \approx 2.3$. This observation supports the idea that charges are distributed over a larger surface area, but the microscopic mechanism is still not fully understood. Unfortunately, there are no ionic strength dependent measurements of D_{T} of PEG.

Figure 4 shows the measured Soret coefficient of PEG-*fd* and the bare *fd*-virus as function of the Debye length. With increasing Debye length S_{T} of the two systems approach each other. This observation supports the hypothesis suggested by fig. 1, that the thermophoretic behavior becomes equal once the electric double layer exceeds the grafted polymer layer. The group of Braun[78] investigated the Soret coefficient of PEG in aqueous salt solutions for various salts of the Hofmeister series. They found that S_{T} was constant and independent of the salt and the ionic strength. Therefore, we assume that the observed Debye length dependence of S_{T} results from the charged *fd*-virus and contains no contribution by the grafted PEG.

This work shows that the thermodiffusion behaviour of colloidal particles can be modified by changes to their surface. However, for our charged colloidal rods, this is only true at high ionic strength. Once the Debye length exceeds a certain value, thermodiffusion of

the particle is ruled by electrostatic effects and the nature of the particle surface seems to become irrelevant. The determined mass fraction of the surface layer of 22% corresponds to a volume fraction of roughly 5%, which explains that the polymeric chains as well as the colloidal rod are in contact with the solvent so that the thermal diffusion coefficients are additive. For this low concentration the thermophoretic behavior of both systems can be described by an analytical theory of charged rods without the need to take inter-particle effects into account. In the case of the grafted virus the calculated surface charge density is lower. The decrease scales with increasing surface area, so that the total charge of the colloid remains constant, which is also expected from the analysis of the charge in the electrophoresis section. Experimentally it is rather difficult to fully resolve the microscopic mechanism of this system. On the other hand, the large virus and the long range interactions make it also badly suited for molecular dynamic simulations.

Acknowledgement

The authors warmly acknowledge useful discussion with Dieter Braun, Wim Briels, Christian Lang, Jutta Luettmer-Strathmann, Gerhard Nägele, Pavlik Lettinga, and Marisol Ripoll. ZW and DN acknowledge support by the International Helmholtz Research School of Biophysics and Soft Matter (IHRS BioSoft).

Supporting Information Available

We estimated the thickness of the PEG layer using various literature results and summarize the equations to determine the effective diameter of a charged rod according to the Onsager theory. Additionally the Debye length as function for all investigated solutions as function of ionic strength and TRIS buffer is listed. Further a summary of the dynamic light scattering results to determine the Stokes Einstein diffusion coefficient D_0 is given.

References

(1) Wienken, C. J.; Baaske, P.; Rothbauer, U.; Braun, D.; Duhr, S. Protein-Binding Assays in Biological Liquids Using Microscale Thermophoresis. *Nat. Commun.* **2010**, *1*, 1–7.

(2) Baaske, P.; Weinert, F. M.; Duhr, S.; Lemke, K. H.; Russell, M. J.; Braun, D. Extreme Accumulation of Nucleotides in Simulated Hydrothermal Pore Systems. *P. Natl. Acad. Sci. USA* **2007**, *104*, 9346–9351.

(3) Niether, D.; Afanasenkau, D.; Dhont, J. K. G.; Wiegand, S. Accumulation of Formamide in Hydrothermal Pores to Form Prebiotic Nucleobases. *P. Natl. Acad. Sci. USA* **2016**, *113*, 4272–4277.

(4) Debuschewitz, C.; Köhler, W. Molecular Origin of Thermal Diffusion in Benzene Plus Cyclohexane Mixtures. *Phys. Rev. Lett.* **2001**, *87*, 055901.

(5) Rauch, J.; Köhler, W. Collective and Thermal Diffusion in Dilute, Semidilute, and Concentrated Solutions of Polystyrene in Toluene. *J. Chem. Phys.* **2003**, *119*, 11977–11988.

(6) Iacopini, S.; Rusconi, R.; Piazza, R. The "Macromolecular Tourist": Universal Temperature Dependence of Thermal Diffusion in Aqueous Colloidal Suspensions. *Eur. Phys. J. E* **2006**, *19*, 59–67.

(7) Ning, H.; Dhont, J. K. G.; Wiegand, S. Thermal-diffusive behavior of a dilute solution of charged colloids. *Langmuir* **2008**, *24*, 2426–2432.

(8) Naumann, P.; Datta, S.; Sottmann, T.; Arlt, B.; Frielinghaus, H.; Wiegand, S. Isothermal Behavior of the Soret Effect in Nonionic Microemulsions: Size Variation by Using Different N-Alkanes. *J. Phys. Chem. B* **2014**, *118*, 3451–3460.

(9) Sehnem, A. L.; Aquino, R.; Campos, A. F. C.; Tourinho, F. A.; Depeyrot, J.; Neto, A.

M. F. Thermodiffusion in Positively Charged Magnetic Colloids: Influence of the Particle Diameter. *Phys. Rev. E* **2014**, *89*, 032308–1–032308–7.

(10) Bringuier, E.; Bourdon, A. Colloid transport in nonuniform temperature. *Phys. Rev. E* **2003**, *67*, 011404.

(11) Dhont, J. Thermodiffusion of Interacting Colloids. I. A Statistical Thermodynamics Approach. *J. Chem. Phys.* **2004**, *120*, 1632–1641.

(12) Parola, A.; Piazza, R. Particle Thermophoresis in Liquids. *Eur. Phys. J. E* **2004**, *15*, 255–263.

(13) Würger, A. Temperature Dependence of the Soret Motion in Colloids. *Langmuir* **2009**, *25*, 6696–6701.

(14) Zhang, M.; Müller-Plathe, F. The Soret Effect in Dilute Polymer Solutions: Influence of Chain Length, Chain Stiffness, and Solvent Quality. *J. Chem. Phys.* **2006**, *125*, 124903.

(15) Artola, P. A.; Rousseau, B. Microscopic Interpretation of a Pure Chemical Contribution to the Soret Effect. *Phys. Rev. Lett.* **2007**, *98*, 125901–1–125901–4.

(16) Galliero, G.; Volz, S. Thermodiffusion in Model Nanofluids by Molecular Dynamics Simulations. *J. Chem. Phys.* **2008**, *128*, 064505.

(17) Lüsebrink, D.; Yang, M.; Ripoll, M. Thermophoresis of Colloids by Mesoscale Simulations. *J. Phys. - Condens. Mat.* **2012**, *24*, 284132.

(18) Yang, M. C.; Ripoll, M. Thermophoretically Induced Flow Field around a Colloidal Particle. *Soft Matter* **2013**, *9*, 4661–4671.

(19) Tan, Z. H.; Yang, M. C.; Ripoll, M. Anisotropic Thermophoresis. *Soft Matter* **2017**, *13*, 7283–7291.

(20) Polyakov, P.; Rossinsky, E.; Wiegand, S. Study of the Soret Effect in Hydrocarbon Chain/Aromatic Compound Mixtures. *J. Phys. Chem. B* **2009**, *113*, 13308–13312.

(21) Hartmann, S.; Wittko, G.; Köhler, W.; Morozov, K. I.; Albers, K.; Sadowski, G. Thermophobicity of Liquids: Heats of Transport in Mixtures as Pure Component Properties. *Phys. Rev. Lett.* **2012**, *109*, 065901–1–065901–4.

(22) De Mezquia, D. A.; Bou-Ali, M. M.; Larranaga, M.; Madariaga, J. A.; Santamaria, C. Determination of Molecular Diffusion Coefficient in N-Alkane Binary Mixtures: Empirical Correlations. *J. Phys. Chem. B* **2012**, *116*, 2814–2819.

(23) Kishikawa, Y.; Wiegand, S.; Kita, R. Temperature Dependence of Soret Coefficient in Aqueous and Nonaqueous Solutions of Pullulan. *Biomacromolecules* **2010**, *11*, 740–747.

(24) Wang, Z.; Kriegs, H.; Wiegand, S. Thermal Diffusion of Nucleotides. *J. Phys. Chem. B* **2012**, *116*, 7463–7469.

(25) Niether, D.; Di Lecce, S.; Bresme, F.; Wiegand, S. Unravelling the Hydrophobicity of Urea in Water Using Thermodiffusion: Implications for Protein Denaturation. *Phys. Chem. Chem. Phys.* **2018**, *20*, 1012–1020.

(26) Eguchi, K.; Niether, D.; Wiegand, S.; Kita, R. Thermophoresis of Cyclic Oligosaccharides in Polar Solvents. *Eur. Phys. J. E* **2016**, *39*, 86.

(27) Niether, D.; Kriegs, H.; Dhont, J. K. G.; Wiegand, S. Peptide Model Systems: Correlation between Thermophilicity and Hydrophilicity. *J. Chem. Phys.* **2018**, *149*.

(28) Sangster, J. Octanol-Water Partition Coefficients of Simple Organic Compounds. *J. Phys. Chem. Ref. Data* **1989**, *18*, 1111–1229.

(29) Kolodner, P.; Williams, H.; Moe, C. Optical Measurement of the Soret Coefficient of Ethanol Water Solutions. *J. Chem. Phys.* **1988**, *88*, 6512–6524.

(30) Polyakov, P.; Wiegand, S. Systematic Study of the Thermal Diffusion in Associated Mixtures. *J. Chem. Phys.* **2008**, *128*, 034505.

(31) Maeda, K.; Shinyashiki, N.; Yagihara, S.; Wiegand, S.; Kita, R. Ludwig-Soret Effect of Aqueous Solutions of Ethylene Glycol Oligomers, Crown Ethers, and Glycerol: Temperature, Molecular Weight, and Hydrogen Bond Effect. *J. Chem. Phys.* **2015**, *143*, 124504.

(32) Blanco, P.; Kriegs, H.; Lettinga, M. P.; Holmqvist, P.; Wiegand, S. Thermal diffusion of a stiff rod-like mutant Y21M fd-virus. *Biomacromolecules* **2011**, *12*, 1602–9.

(33) Wang, Z.; Kriegs, H.; Buitenhuis, J.; Dhont, J. K. G.; Wiegand, S. Thermophoresis of Charged Colloidal Rods. *Soft Matter* **2013**, *9*, 8697–8704.

(34) Sehnem, A. L.; Neto, A. M. F.; Aquino, R.; Campos, A. F. C.; Tourinho, F. A.; Depeyrot, J. Temperature Dependence of the Soret Coefficient of Ionic Colloids. *Phys. Rev. E* **2015**, *92*, 042311–1–042311–8.

(35) Dhont, J. K. G.; Wiegand, S.; Duhr, S.; Braun, D. Thermodiffusion of charged colloids: Single-particle diffusion. *Langmuir* **2007**, *23*, 1674–1683.

(36) Dhont, J. K. G.; Briels, W. J. Single-Particle Thermal Diffusion of Charged Colloids: Double-Layer Theory in a Temperature Gradient. *Eur. Phys. J. E* **2008**, *25*, 61–76.

(37) Würger, A. Transport in Charged Colloids Driven by Thermoelectricity. *Phys. Rev. Lett.* **2008**, *101*, 108302–1–108302–4.

(38) Majee, A.; Würger, A. Collective Thermoelectrophoresis of Charged Colloids. *Phys. Rev. E* **2011**, *83*.

(39) Golestanian, R. Collective Behavior of Thermally Active Colloids. *Physical Review Letters* **2012**, *108*, 038303–1–038303–5.

(40) Burelbach, J.; Frenkel, D.; Pagonabarraga, I.; Eiser, E. A Unified Description of Colloidal Thermophoresis. *Eur. Phys. J. E* **2018**, *41*.

(41) Römer, F.; Wang, Z.; Wiegand, S.; Bresme, F. Alkali Halide Solutions under Thermal Gradients: Soret Coefficients and Heat Transfer Mechanisms. *J. Phys. Chem. B* **2013**, *117*, 8209–8222.

(42) Pusey, P. N.; van Megen, W. Phase-Behavior of Concentrated Suspensions of Nearly Hard Colloidal Spheres. *Nature* **1986**, *320*, 340–342.

(43) Yethiraj, A. Tunable Colloids: Control of Colloidal Phase Transitions with Tunable Interactions. *Soft Matter* **2007**, *3*, 1099–1115.

(44) Duhr, S.; Braun, D. Why molecules move along a temperature gradient. *P. Natl. Acad. Sci. USA* **2006**, *103*, 19678–19682.

(45) Vigolo, D.; Brambilla, G.; Piazza, R. Thermophoresis of Microemulsion Droplets: Size Dependence of the Soret Effect. *Phys. Rev. E* **2007**, *75*, 040401.

(46) Putnam, S. A.; Cahill, D. G.; Wong, G. C. L. Temperature Dependence of Thermodiffusion in Aqueous Suspensions of Charged Nanoparticles. *Langmuir* **2007**, *23*, 9221–9228.

(47) Braibanti, M.; Vigolo, D.; Piazza, R. Does Thermophoretic Mobility Depend on Particle Size? *Phys. Rev. Lett.* **2008**, *100*, 108303–1–108303–4.

(48) Wongsuwarn, S.; Vigolo, D.; Cerbino, R.; Howe, A. M.; Vailati, A.; Piazza, R.; Cicuta, P. Giant Thermophoresis of Poly(N-Isopropylacrylamide) Microgel Particles. *Soft Matter* **2012**, *8*, 5857–5863.

(49) Naumann, P.; Becker, N.; Datta, S.; Sottmann, T.; Wiegand, S. Soret Coefficient in Nonionic Microemulsions: Concentration and Structure Dependence. *J. Phys. Chem. B* **2013**, *117*, 5614–5622.

(50) de Gans, B.-J.; Kita, R.; Wiegand, S.; Luettmer Strathmann, J. Unusual Thermal Diffusion in Polymer Solutions. *Phys. Rev. Lett.* **2003**, *91*, 245501.

(51) Kita, R.; Wiegand, S.; Luettmer Strathmann, J. Sign change of the Soret coefficient of poly(ethylene oxide) in water/ethanol mixtures observed by TDFRS. *J. Chem. Phys.* **2004**, *121*, 3874–3885.

(52) Wind, B.; Killmann, E. Adsorption of Polyethylene Oxide on Surface Modified Silica Stability of Bare and Covered Particles in Suspension. *Colloid. Polym. Sci.* **1998**, *276*, 903–912.

(53) Giesbers, M.; Kleijn, J. M.; Fleer, G. J.; Stuart, M. A. C. Forces between Polymer-Covered Surfaces: A Colloidal Probe Study. *Colloids Surf. A* **1998**, *142*, 343–353.

(54) Wen, Y. H.; Lin, P.-C.; Lee, C. Y.; Hua, C. C.; Lee, T.-C. Reduced Colloidal Repulsion Imparted by Adsorbed Polymer of Particle Dimensions. *J Colloid Interface Sci.* **2010**, *349*, 134–141.

(55) Joksimovic, R.; Prevost, S.; Schweins, R.; Appavou, M. S.; Gradzielski, M. Interactions of Silica Nanoparticles with Poly(Ethylene Oxide) and Poly(Acrylic Acid): Effect of the Polymer Molecular Weight and of the Surface Charge. *J. Colloid Interface Sci.* **2013**, *394*, 85–93.

(56) Dogic, Z.; Fraden, S. Ordered phases of filamentous viruses. *Curr. Opin. Colloid Interface Sci.* **2006**, *11*, 47–55.

(57) Kang, K.; Dhont, J. K. G. Electric-field induced transitions in suspensions of charged colloidal rods. *Soft Matter* **2010**, *6*, 273–286.

(58) Ripoll, M.; Holmqvist, P.; Winkler, R. G.; Gompper, G.; Dhont, J. K. G.; Lettinga, M. P. Attractive Colloidal Rods in Shear Flow. *Phys. Rev. Lett.* **2008**, *101*, 168302–1–168302–4.

(59) Purdy, K. R. Liquid Crystal Phase Transitions of Monodisperse and Bidisperse Suspensions of Rodlike Colloidal Virus. Ph.D. thesis, Brandeis University, 2004.

(60) Chan, J.; Popov, J. J.; Kolisnek-Kehl, S.; Leaist, D. G. Soret coefficients for aqueous polyethylene glycol solutions and some tests of the segmental model of polymer thermal diffusion. *J. Solution Chem.* **2003**, *32*, 197–214.

(61) Klein, M.; Wiegand, S. The Soret effect of mono-, di- and tri-glycols in ethanol. *Physical Chemistry Chemical Physics* **2011**, *13*, 7059–7063.

(62) Wang, Z.; Afanasenkau, D.; Dong, M.; Huang, D.; Wiegand, S. Molar Mass and Temperature Dependence of the Thermodiffusion of Polyethylene Oxide in Water/Ethanol Mixtures. *J. Chem. Phys.* **2014**, *141*, 064904–1–064904–7.

(63) Israelachvili, J. The Different Faces of Poly(Ethylene Glycol). *Proceedings of the National Academy of Sciences of the United States of America* **1997**, *94*, 8378–8379.

(64) Dormidontova, E. E. Role of Competitive PEO-Water and Water-Water Hydrogen Bonding in Aqueous Solution Peo Behavior. *Macromolecules* **2002**, *35*, 987–1001.

(65) Onsager, L. The effects of shape on the interaction of colloidal particles. *Ann. N.Y. Acad. Sci* **1949**, *51*, 627–659.

(66) Zhang, Z.; Buitenhuis, J.; Cukkemane, A.; Brocker, M.; Bott, M.; Dhont, J. K. G. Charge Reversal of the Rodlike Colloidal *fd* Virus through Surface Chemical Modification. *Langmuir* **2010**, *26*, 10593–10599.

(67) Dhont, J. Thermodiffusion of Interacting Colloids. II. A Microscopic Approach. *J. Chem. Phys.* **2004**, *120*, 1642–1653.

(68) Ning, H.; Buitenhuis, J.; Dhont, J. K. G.; Wiegand, S. Thermal Diffusion Behavior of Hard-Sphere Suspensions. *J. Chem. Phys.* **2006**, *125*, 204911.

(69) Dhont, J. K. G.; van Bruggen, M. P. B.; Briels, W. J. Long-Time Self-Diffusion of Rigid Rods at Low Concentrations:A Variational Approach. *Macromolecules* **1999**, *32*, 3809–3816.

(70) Song, L.; Kim, U. S.; Wilcoxon, J.; Schurr, J. M. Dynamic Light-Scattering from Weakly Bending Rods - Estimation of the Dynamic Bending Rigidity of the M13 Virus. *Biopolymers* **1991**, *31*, 547–567.

(71) Sambrook, J.; Russell, D. *Molecular Cloning: A Laboratory Manual*; Cold Spring Harbor Lab Press: New York, 2001.

(72) Dogic, Z.; Fraden, S. Development of model colloidal liquid crystals and the kinetics of the isotropic-smectic transition. *Phil. Trans. R. Soc. Lond. A* **2001**, *359*, 997–1014.

(73) Kramer, H.; Graf, C.; Hagenbuchle, M.; Johner, C.; Martin, C.; Schwind, P.; Weber, R. Electrooptic Effects of Aqueous Fd-Virus Suspensions at Very-Low Ionic-Strength. *J. Phys. II* **1994**, *4*, 1061–1074.

(74) Hunter, R. J. *Colloid Science*; Zeta Potential in Colloid Science; Academic Press, 1981.

(75) Buitenhuis, J. Electrophoresis of Fd-Virus Particles: Experiments and an Analysis of the Effect of Finite Rod Lengths. *Langmuir* **2012**, *28*, 13354–13363.

(76) Nägele, G. *The physics of colloidal soft matter*; Institute of Fundamental Technological Research, Polish academy of Science: Warsaw, 2004; Vol. 14; pp 1–181.

(77) McPhie, M. G.; Nägele, G. Long-time self-diffusion of charged colloidal particles: Electrokinetic and hydrodynamic interaction effects. *J. Chem. Phys.* **2007**, *127*, 034906.

(78) Braun, D. talk at the 13th International Meeting on Thermodiffusion in London, 2018.

Graphical TOC Entry